

Crystal Hartree-Fock calculations for La_2NiO_4 and La_2CuO_4

Yen-Sheng Su, T. A. Kaplan, and S. D. Mahanti

*Center for Fundamental Materials Research and Department of Physics and Astronomy, Michigan State University,
East Lansing, Michigan 48824*

J. F. Harrison

*Center for Fundamental Materials Research and Department of Chemistry, Michigan State University, East Lansing, Michigan 48824
(Received 4 June 1998)*

Ground-state properties of La_2NiO_4 and the isostructural compound La_2CuO_4 , the parent material of some high- T_c superconductors, have been calculated using the Hartree-Fock approximation (HFA). To our knowledge, this is the first report in the literature in which calculations for these two materials are done for an infinite crystal using the HFA. The results show that both the nickelate and cuprate are antiferromagnetic (AFM) insulators, in agreement with experiments. The character of the highest occupied band in the cuprate is found to be in-plane O $2p_{x,y}$ strongly mixed with Cu $3d_{x^2-y^2}$, agreeing with the hypotheses of most Hubbard models for this problem. The spin densities show rather localized peaks with approximate cubic symmetry at Ni sites (due to two singly occupied e_g orbitals) or approximate fourfold symmetry at Cu sites (due to $d_{x^2-y^2}$), and are small elsewhere. The corresponding form factor agrees rather closely with our earlier cluster calculations for the nickelate, while differing appreciably in the cuprate. We speculate on the reason for this. The results for the cuprate are consistent with magnetic neutron-scattering experiments: The shape of the form factor is in overall qualitative agreement with that measured on a sample of questionable stoichiometry; for a sample with presumably good stoichiometry, on which only one Bragg peak was measured, the absolute intensity is in remarkably good agreement with our calculated result. The latter includes the well-known correction for zero-point or quantum spin fluctuations. However, the shape of the form factor for the nickelate is in serious disagreement with experiment. We also calculated the energy splitting between AFM and ferromagnetic states, and, for both materials, found the corresponding Heisenberg exchange parameter J to be of the correct order of magnitude (about a factor of 3 smaller than the experimental values). The calculated J value for the cuprate is close to the result of a recent cluster Hartree-Fock calculation. We discuss the determination of J in density-functional theories, as well as in the HFA, in the Appendix. [S0163-1829(99)02115-3]

I. INTRODUCTION AND METHODS

La_2NiO_4 and La_2CuO_4 , which have essentially the same crystal structure, have attracted considerable theoretical and experimental research efforts, especially since the latter was found to become a high- T_c superconductor when properly doped with Sr or Ba.¹ Above their respective structural transition temperatures T_S , both materials are in a tetragonal structure [space group $D_{4h}^{17}(I4/mmm)$; see Fig. 1]. Below T_S , they are slightly distorted to an orthorhombic structure. Each of them is an antiferromagnetic (AFM) insulator below a Néel temperature $T_N (< T_S)$, and is a paramagnetic (PM) insulator above T_N .

The past theoretical studies of these two materials can be broadly classified into two categories. The first one is density-functional calculations executed on the crystals. This sort of approach only achieved partial success, and failed to predict certain properties of the materials. For instance, local-spin-density-approximation (LSDA) calculations incorrectly predicted La_2CuO_4 to be a PM metal¹ and La_2NiO_4 to be an AFM metal.² After 1990, several modifications were made to the LSDA to produce AFM insulating solutions, like self-interaction-corrected LSDA and LSDA+U.^{3,4} However, since the modifications are somewhat *ad hoc*, whether the modified LSDA approaches still fall into the *ab initio* regime or not is arguable.

The second category is cluster calculations. This category itself can be further divided into two subsets: single-magnetic-ion cluster (SMIC) calculations and multi-magnetic-ion cluster (MMIC) calculations. The SMIC calculations were aimed at obtaining the neutron-scattering form factors of the crystals⁵ and hyperfine properties.⁶ A more detailed description of this approach will be given in Sec. II, when we come to the comparison of results of the SMIC calculations with the results of our present work. Note that, since the cluster in the SMIC calculations contains only one magnetic ion, the AFM ground state of the crystals must be assumed *a priori*, and quantities such as the Heisenberg exchange parameter J cannot be extracted from the calculations. On the other hand, MMIC calculations⁷⁻¹⁰ have given information about J .

The present calculations were done using the program CRYSTAL95,¹¹ which is designed to do Hartree-Fock (HF) calculations on infinite crystalline materials, using linear-combination-of-atomic-orbital basis sets. Clearly, the crystal Hartree-Fock approximation (HFA) falls outside the two categories mentioned above, and thus may provide useful supplementary information. The crystal HFA has recently been applied to a number of AFM Mott insulators including MnO, NiO,¹² KNiF₃,¹³ KCuF₃,¹⁴ and CaCuO₂.¹⁵ These were successful in that they gave the materials to be insulators (vs metals), to be antiferromagnets (vs ferro- or paramagnets);

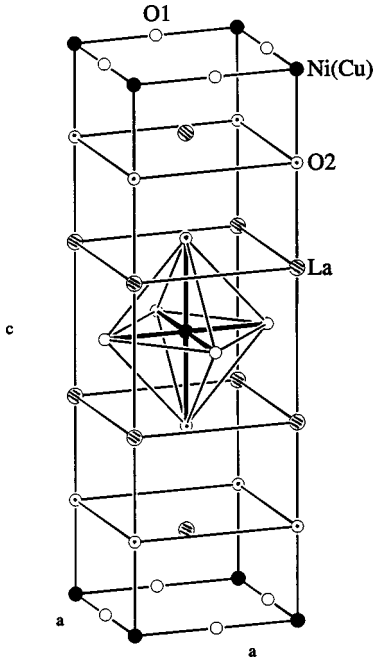


FIG. 1. The centered-tetragonal structure of La_2NiO_4 and La_2CuO_4 .

they also gave energy differences between the various magnetic states in semiquantitative agreement with experiment. In this paper, in addition to these considerations, we will compare the spin density with neutron-diffraction experiments. Our major emphasis is on the ground-state properties, although some discussion of band structure (one-electron energies, and the nature of one-electron states) is presented.

In this work, we use the centered tetragonal crystal structures with lattice constants taken from experimental data.¹⁶ $a = 3.855$ and $c = 12.652$ for La_2NiO_4 , and $a = 3.7793$ and $c = 13.226$ for La_2CuO_4 (in units of \AA). The basis sets of O, Ni, and Cu are taken from Ref. 17, which are especially designed for crystal calculations. (Note that the usual basis sets used in molecular and cluster calculations are often too diffuse for crystal calculations; they may cause nonconvergence or a very slow convergence rate with not much improvement in the accuracy to the result one might obtain using tighter basis sets.¹¹) Since La is a heavy atom (atomic number 57), relativistic effects are not negligible for the inner shell electrons. In addition, an atomic basis set for La suitable for crystal calculation is not available in the literature. We thus used the effective core potential (ECP) calculated by Hay and Wadt¹⁸ for the La^{+3} -ion core,¹⁹ where the relativistic effect of the inner-shell electrons is supposed to have been taken into account. In Hay and Wadt's papers, basis sets for valence electrons designed for use with the ECPs were also given. However, they are so diffuse that they cause a numerical problem in the crystal HF calculation. Thus La was treated in the present work as a bare La^{+3} ion, and represented by the Hay and Wadt large core ECP, no valence orbitals (therefore no valence electrons) being attached to it. We did test the significance of the bare La^{+3} core approximation to some extent by adding a d shell (consisting of a single, optimized, Gaussian exponent) to the La^{+3} and seeing how it affected the results. It turned out that about 0.45 electron per La gathered into the added shell. Accompanying

that, the total energy per formula unit (including one Ni or Cu) changed by about 4.5 eV. However, the shape of the occupied bands and the spin density changed negligibly, and the energy difference between ferromagnetic (FM) and AFM solutions, which is around 36 meV, varied by only about 1.4 meV. The insensitivity of the FM-AFM energy difference to variation of the outer shells of basis sets was also observed for other materials.¹³ The properties that are only slightly affected by the bare La^{+3} core approximation are the main focus in this paper.

II. RESULTS

A. Heisenberg exchange parameter J

Our results show that both La_2NiO_4 and La_2CuO_4 are AFM insulators, in agreement with experiments. The FM solutions also exist for both materials, with higher energy. The energy difference per formula unit between FM and AFM states is 36.9 meV for La_2NiO_4 and 36.1 meV for La_2CuO_4 . It is a common and long-standing practice^{20,21,12-14,7} to map energies of FM and AFM electronic states to the mean-field approximation for the nearest-neighbor Heisenberg Hamiltonian H_{Heis} . This is done for materials such as these, where H_{Heis} is known to accurately describe the low-lying excitations,^{20,22} and leads to an estimate of the Heisenberg exchange parameter J . In the Appendix, we give a rationale for doing the mapping in HF calculations, while pointing out a potential inconsistency if the same procedure is used in approximate density-functional theories.

To proceed then with the determination of J , the Heisenberg Hamiltonian is

$$H_{\text{Heis}} = J \sum_{\langle i,j \rangle} \vec{s}_i \cdot \vec{s}_j, \quad (1)$$

the summation going over each nearest neighbor pair $\langle i,j \rangle$ of magnetic ions, taken once. We equate the calculated FM-AFM energy difference in the HFA to the corresponding FM-AFM energy difference in the mean-field approximation of Eq. (1), and thus define the Heisenberg J in the HFA, J_{HF} , as follows:

$$\Delta E_{\text{HF}} = (2J_{\text{HF}}s^2) \left(\frac{NZ}{2} \right). \quad (2)$$

ΔE_{HF} is the FM-AFM energy difference for the whole crystal in the HFA, N is the number of magnetic ions, s is the spin of each site (1 for Ni and $\frac{1}{2}$ for Cu), and Z is the coordination number. Equation (2) (with J instead of J_{HF}) appears elsewhere⁷⁻¹⁰ for dimers where $N=2$ and $Z=1$, but the claim in some of the references that this gives the *correct* or *exact* J is not warranted in general (see the Appendix). Since the interactions within a CuO_2 plane are much stronger than the interplanar ones, we take $Z=4$. It turns out that J is 9.2 meV for La_2NiO_4 and 36.1 meV for La_2CuO_4 . The La_2CuO_4 result agrees with an embedded-cluster calculation using the HFA,⁷ which gives 37.8 meV, strengthening the suggestion⁷⁻¹⁰ that J appears to be a rather local property. These values are to be compared with the experimental data, which give 30 meV for La_2NiO_4 ,^{23,24} and 134 (neutron) or 128 (Raman) meV for La_2CuO_4 .^{25,26} Although our results are

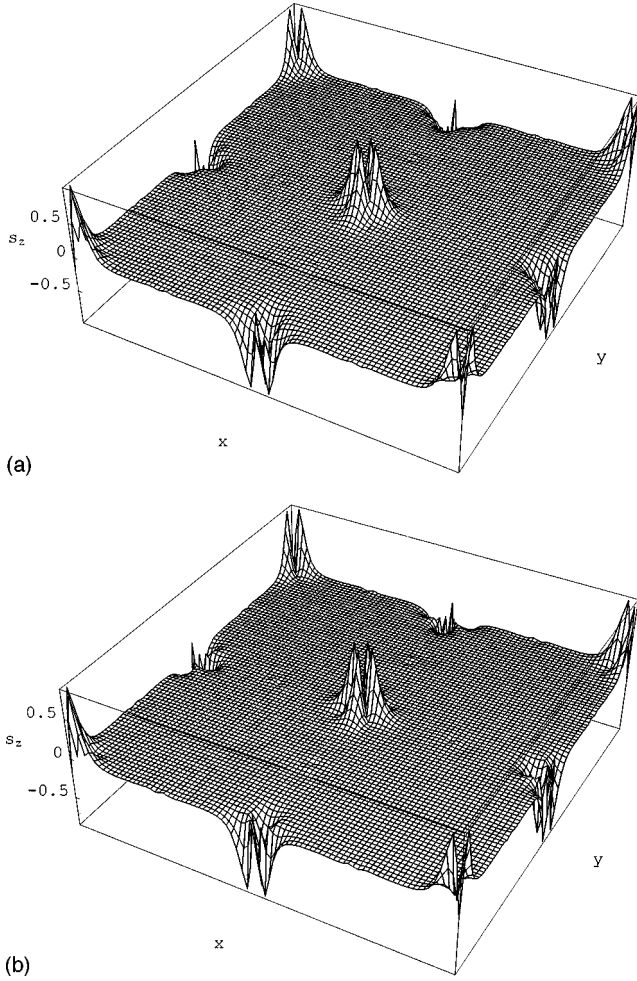


FIG. 2. The spin density in the magnetic ion-oxygen plane [(001) plane]: (a) La_2NiO_4 , AFM; (b) La_2CuO_4 , AFM. The range of the basal plane in the graphics is $2a$ (a is the lattice constant) in each direction, and is centered at one magnetic ion. The vertical axis is in atomic units (same as Fig. 3 in the following).

about a factor of 3 too small, it actually is remarkable to be so close, since we are picking up the small difference between the FM and AFM energies with each on the order of 4000 Hartrees. (So it is at an accuracy of about one out of a million.) Similar underestimates for J using the HFA were found for other materials.¹²⁻¹⁴

B. Spin density and spin form factor

Spin-density maps on the perovskite magnetic ion-oxygen layer [(001) plane] are given in Fig. 2 for both materials. The x - y plane of the graphs matches the NiO_2 (CuO_2) plane, and includes 3×3 magnetic ion sites. The large peaks on the graphs coincide with the locations of the magnetic ions. The sign of the spin density alternates from one site to another, a manifestation of the AFM character of the systems. The magnitudes of spin density around oxygens, which are half-way between each nearest-neighbor pair of magnetic ions, are extremely small, as expected. Every peak in the graphs has an approximate fourfold symmetric shape, a result of the singly occupied $d_{x^2-y^2}$ orbital. Although Figs. 2(a) (for La_2NiO_4) and 2(b) (for La_2CuO_4) resemble each other very much, a characteristic difference between the spin densities

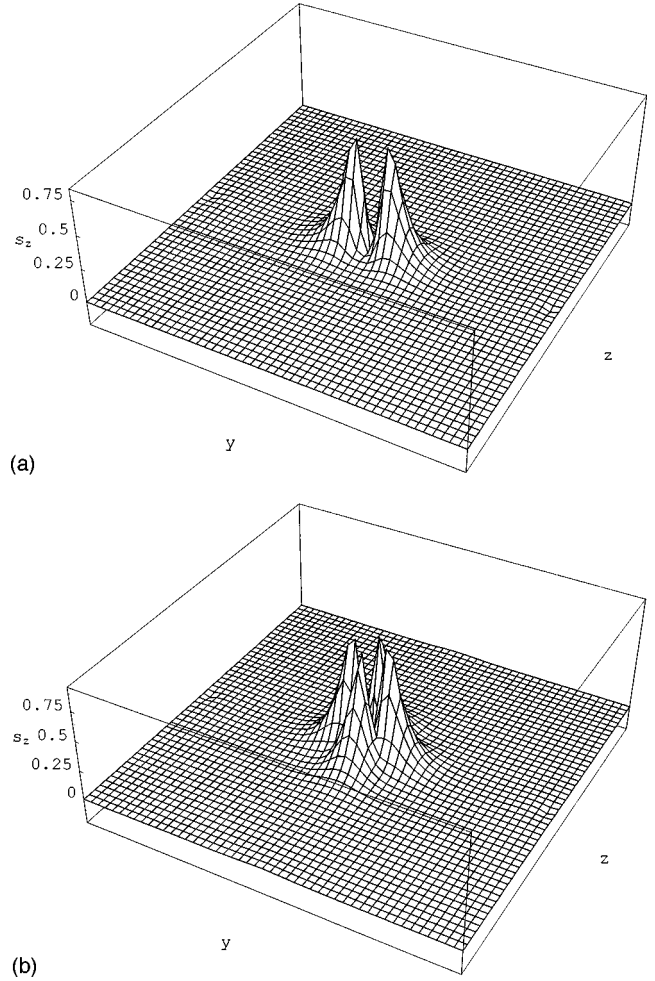


FIG. 3. The spin density in the (100) plane: (a) La_2NiO_4 , AFM; (b) La_2CuO_4 , AFM. The range of the basal plane in the graphics is a in each direction, and is centered on one magnetic ion. The labels of the two axes of the basal plane refer to the y and z directions in the conventional tetragonal lattice coordinates.

of these two materials does exist, and can be seen in a tomograph of other directions. For instance, Fig. 3 shows the spin-density tomographs of these two materials in the (100) plane passing through a magnetic ion. For this plane, the peak in the graph of La_2NiO_4 still has four lobes, while the peak in the graph of La_2CuO_4 has only two lobes aligned in the y direction. This is expected because each copper in La_2CuO_4 has only a singly occupied $d_{x^2-y^2}$, while each nickel in La_2NiO_4 has a singly occupied $d_{x^2-y^2}$ and a singly occupied $d_{3z^2-r^2}$, which together give a spin distribution with cubic symmetry (small distortions from cubic symmetry are caused by the surroundings). Later on we will see that this difference in spin densities leads to characteristically different spin form factors for these two materials.

Spin density is connected to elastic neutron scattering experiments, where the scattering amplitude is proportional to the Fourier transform of the spin density. It has been shown⁵ that, for the single-band Hubbard model, assuming small hopping t compared to the repulsion U , the Fourier transform of the spin density is

$$s(\vec{k}) = \langle s_z \rangle_{\text{Heis}} F(\vec{k}) f(\vec{k}) [1 + O((t/U)^2)]. \quad (3)$$

Here $\langle s_z \rangle_{\text{Heis}}$ is the expectation value of the spin at a site (an up site) in the (spontaneously) symmetry-broken ground state of the corresponding Heisenberg model. $f(\vec{k})$, the form factor, is the Fourier transform of $1/s$ times the HF spin density over a nonmagnetic unit cell centered at a magnetic ion, where s is the spin quantum number for the free ion (1 for Ni^{+2} and $\frac{1}{2}$ for Cu^{+2}). This implies $f(0) = 1$. $F(\vec{k})$ is given as

$$F(\vec{k}) = \frac{1}{N} \sum_{\vec{R}} e^{-i(\vec{k} - \vec{k}_A) \cdot \vec{R}}, \quad (4)$$

where \vec{R} runs over all the Bravais lattice vectors, N is the total number of sites, and \vec{k}_A is an antiferromagnetic wave vector [e.g., for the square lattice with lattice constant a , \vec{k}_A is $(\pi/a, \pi/a)$]. The correction term $O[(t/U)^2]$ is negligible for the cuprate⁵ and, we expect, for the nickelate.²⁷ Although the derivation of Eq. (3) is somewhat lengthy, the result is physically understandable. $\langle s_z \rangle_{\text{Heis}}$ accounts for the quantum spin fluctuations (QSF's) in the Heisenberg-model ground state, and is just an overall scale factor. $F(\vec{k})$ accounts for the occurrence of the Bragg peaks. $f(\vec{k})$ gives the relative sizes of the Bragg peaks, and conveys detailed information about the spin density $s(\vec{r})$ in the unit cell. Equation (3) is discussed further in Sec. III.

In an earlier work⁵ of our group, SMIC calculations on several AFM insulating compounds including La_2NiO_4 and La_2CuO_4 were carried out, and the obtained spin densities were compared with experiments based on Eq. (3). The results agreed extremely well for KNiF_3 and NiO ; for La_2CuO_4 they gave rough overall agreement for the shape of $f(\vec{k})$ (for a sample well off stoichiometry). Only in the case of La_2NiO_4 did the results show a serious qualitative disagreement with experiment.²⁸ This disagreement provided a strong part of our motivation for the present study.

Thus the Fourier transform of the spin density from the crystal HF calculations was performed. The resulting form factors at the k values for the magnetic Bragg peaks are shown in Fig. 4.

Note that if the spin density is spherically symmetric, all the data will fall on a smooth curve. In Fig. 4(b), the form factor of La_2CuO_4 , the data separate into several branches, indicating that the form factor varies dramatically in different directions of \vec{k} . This is understood as due to the asphericity of the Cu $d_{x^2-y^2}$ orbital of the unpaired electron, as first pointed out by Shamoto *et al.*²⁹ On the other hand, in the Ni compound both e_g states are singly occupied, giving a nearly cubic spin density, and thus $s(\vec{r})$ is closer to spherical. Indeed, the corresponding form factor [Fig. 4(a)] reveals no obvious branches.

Our present results are compared to the previous cluster calculations and to experiments in Fig. 5. Note that Fig. 5(a) for the nickelate shows the Bragg scattering amplitude (in units of μ_B), and Fig. 5(b) for the cuprate shows the form factor. In Fig. 5(a), the Bragg scattering amplitude $g\langle s_z \rangle_{\text{Heis}}f(\vec{k})$ is calculated using $g = 2.29$ (Ref. 30) and $\langle s_z \rangle_{\text{Heis}} = 0.8$ from the spin-wave theory.³¹ The two theoretical results agree with each other very well; however, both disagree qualitatively with experiment. In view of the very

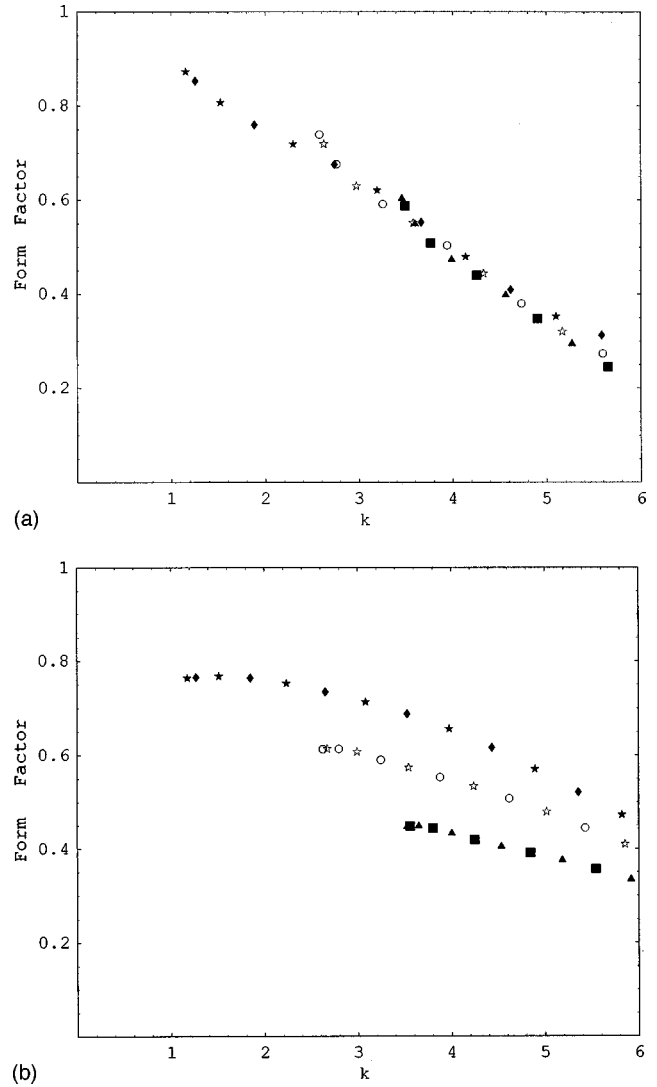


FIG. 4. The spin form factor: (a) La_2NiO_4 , AFM; (b) La_2CuO_4 ; AFM. The horizontal axis is the magnitude of \vec{k} , in units of inverse \AA . The black stars are for the family of $(\frac{1}{2}, -\frac{1}{2}, l)$ Bragg peaks, diamonds for $(\frac{1}{2}, \frac{1}{2}, l)$, circles for $(\frac{1}{2}, \frac{3}{2}, l)$, empty stars for $(\frac{1}{2}, -\frac{3}{2}, l)$, triangles for $(\frac{3}{2}, -\frac{3}{2}, l)$, and squares for $(\frac{3}{2}, \frac{3}{2}, l)$, where the three components of the triple numbers are in units of $2\pi/a$, $2\pi/a$, and $2\pi/c$, respectively. With our choice of coordinate system, for the Bragg peaks the sum of the three components of each triple number must be an even integer.

good agreement between theory and experimental results for several other compounds like KNiF_3 and NiO ,⁵ it seems odd that the theory would be so far off from experiments for the case of La_2NiO_4 . The agreement between the cluster and the crystal calculations ensures that the theoretical results are calculation-error free, excluding one possible source of the discrepancy between theory and experiment. Then, logically, more independent experiments are called for to cross-check with the single existing experimental work on a presumably stoichiometric sample.^{28,32} We should note that the plot in Fig. 5(a) is on an absolute scale; thus the agreement between theory and experiment at large k might be significant.³³

For the cuprate [Fig. 5(b)], the experimental form factor data³⁴ have been scaled to give the least-square fit to the crystal HF result. It has been argued^{35,5} that the moment (and

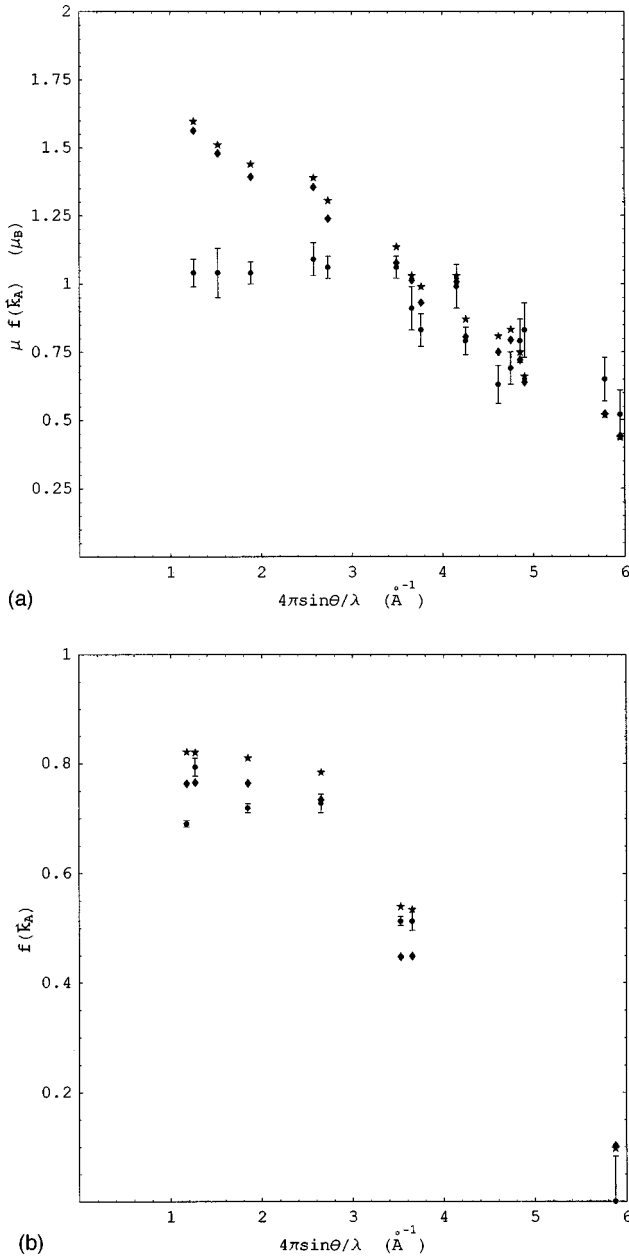


FIG. 5. Comparison of the crystal and cluster calculations with experiments: (a) Bragg scattering amplitude for La_2NiO_4 . (b) Spin form factor for La_2CuO_4 . The diamonds are for the crystal, stars for the cluster, and circles with error bars for the experimental data. Note that in (b) the experimental data have been scaled to make the least-square fit to the crystal results.

Néel temperature) should be maximum at the stoichiometric compound; the main experimental question here is the oxygen content.^{36,37} Since the experimental “moment” in Ref. 34 is appreciably smaller than that of other samples,³⁶ we expect the one used to measure the form factor shown is far from being stoichiometric. Therefore, only comparison of the “shape” of the form factor might be sensible. It is seen that the overall shape is in rough agreement with theory.

For a test of the absolute value of our calculated spin density, we consider the sample with the highest “moment,” 0.6 ± 0.05 Bohr magnetons (with a Néel temperature of 298 K).³⁶ As discussed in Ref. 5, the “moment” (called *moment* in that reference) defined by the experimentalists is the am-

TABLE I. Comparison of the crystal HF approximation, the cluster HF approximation, and the experiment results of the spin form factor of KNiF_3 . The first row shows the indices of the three Bragg peaks measured in experiment. The components of the indexing are in units of $2\pi/a$, a = lattice constant.

	$(\frac{1}{2} \frac{1}{2} \frac{1}{2})$	$(\frac{3}{2} \frac{1}{2} \frac{1}{2})$	$(\frac{3}{2} \frac{3}{2} \frac{1}{2})$
Crystal HF	0.813	0.679	0.554
Cluster HF	0.807	0.683	0.564
Experiment	0.783 ± 0.018	0.672 ± 0.015	0.553 ± 0.013

plitude $g\langle s(\vec{k}) \rangle$ at the Bragg peak with the smallest k , divided by 0.835 (the form factor of K_2CuF_4 , interpolated for the k value appropriate for the cuprate being measured³⁶); g is the usual g factor, $\cong 2.2$ for the cuprate. Multiplying the above “moment” by 0.835 yields $g\langle s(\vec{k}) \rangle_{\text{exp}} = 0.50 \pm 0.04$. Using our calculated HF value of $f(\vec{k}) = 0.763$, $\langle s_z \rangle_{\text{Heis}} = 0.3$ for the square lattice (appropriate to a CuO_2 plane),³¹ and $g = 2.2$, Eq. (3) gives $g\langle s(\vec{k}) \rangle_{\text{theor}} = 0.504$. This exact agreement is surely fortuitous. In fact a sample with a slightly higher T_N (325 K) has been reported³⁸ as being highly stoichiometric. Unfortunately an absolute magnetic Bragg intensity measurement (which would yield, e.g., a value of the “moment”) was not reported on this sample. Judging from the increase in “moment” with T_N shown in Ref. 36, the experimental amplitude will be larger than the 0.5 quoted above. Nevertheless, this agreement between theory and experiment suggests that the HF approach, corrected for quantum spin fluctuations, gives a very good account of the ground-state spin density. It is clearly important to have the absolute intensities at several Bragg peaks measured on an excellent sample like that of Ref. 38, for comparison with our calculations.

It is noted that an appreciable discrepancy between the crystal and cluster HF results exists. This is interesting in view of the very good agreement between the two theoretical calculations for the nickelate, as shown in Fig. 5(a). We believe that the larger covalence in the cuprate is the cause of this discrepancy. Indeed, we performed the integration of the HF spin density over a Wigner-Seitz cell on the magnetic ion sublattice, as a measure of the ordered spin per magnetic ion (without QSF’s), on both materials. We found 0.926 for the nickelate and 0.421 for the cuprate. In comparison with the free magnetic ion spin (1 for Ni^{+2} and $\frac{1}{2}$ for Cu^{+2}), we see a 7.36% reduction for the nickelate and 15.8% reduction for the cuprate.³⁹ This reduction is evidence of the covalence between Ni (Cu) and oxygen.^{40,41} The finding here of appreciably less covalence in the nickelate strongly suggests that the original explanation²⁸ of the extreme flattening of the form factor at small k as being due to strong covalence may not be correct.⁴²

As one further check on the accuracy of our crystal calculations, we considered another Ni compound, KNiF_3 , where the cluster approach agreed excellently with experiment.^{5,30} Taking $\langle s_z \rangle_{\text{Heis}} = 0.92$ from the spin-wave theory,³¹ we summarize the results for the amplitude $\langle s(\vec{k}) \rangle$ at the three Bragg peaks measured in Table I. It is apparent that both the crystal and cluster results are slightly larger than the experimental data. However, if we took $\langle s_z \rangle_{\text{Heis}}$

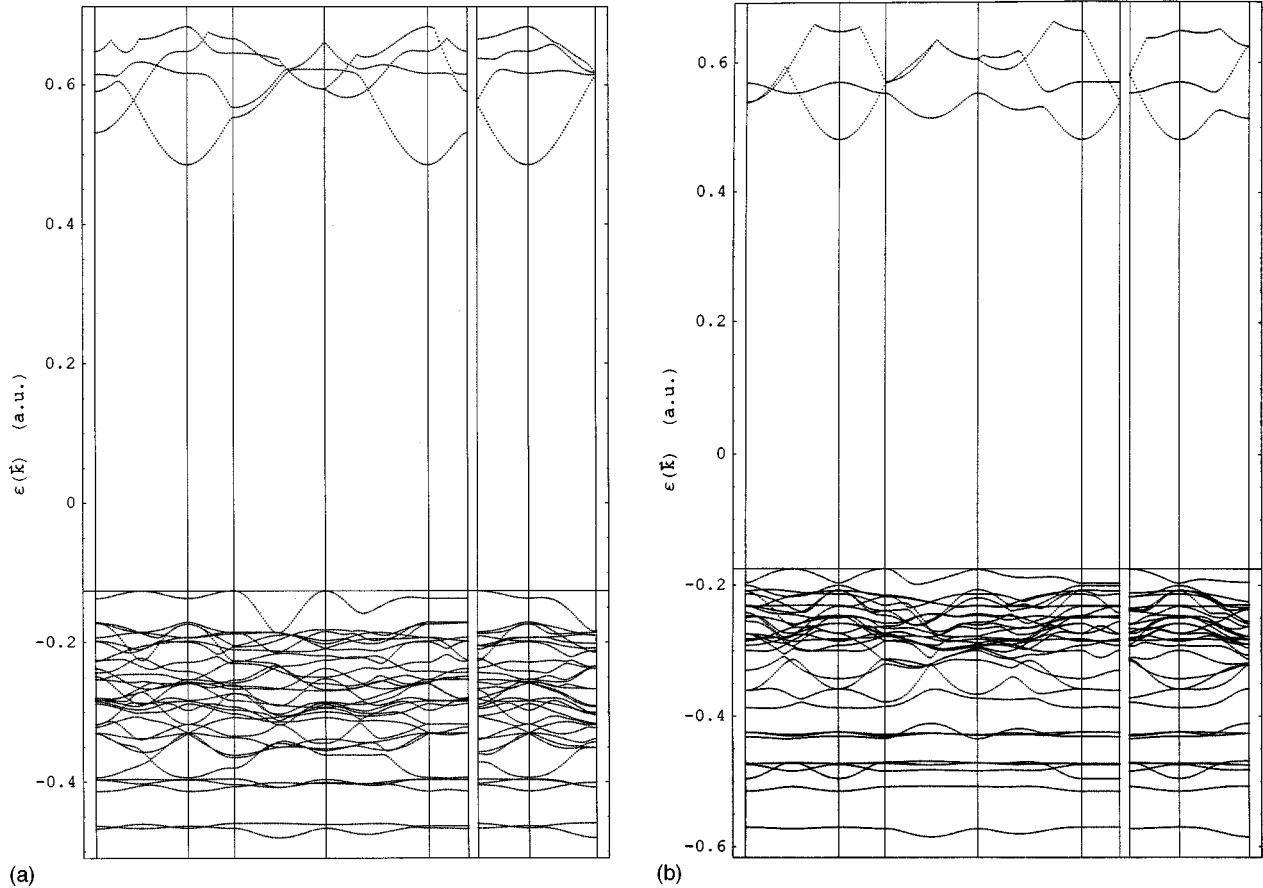


FIG. 6. The band structure: (a) La_2NiO_4 ; AFM; (b) La_2CuO_4 ; AFM. The band structures of the spin-up and -down states are the same (because of the antiferromagnetism), so the figure shown here is for either one. The (vertical) ε axis is in units of Hartrees. The (horizontal) k axis goes through two contiguous paths: $(\frac{1}{2} \frac{1}{2} 0) \rightarrow (000) \rightarrow (\frac{1}{4} \frac{1}{4} 0) \rightarrow (\frac{3}{4} \frac{1}{4} 0) \rightarrow (000) \rightarrow (001)$ and $(\frac{1}{4} \frac{1}{4} \frac{1}{2}) \rightarrow (000) \rightarrow (\frac{1}{2} 0 \frac{1}{2})$. For the convention of the triple numbers, see the caption of Fig. 4. The horizontal line inside each graph indicates the Fermi energy.

$=0.9$, both of them predict the experimental data to within the error bars. It should be remembered that the spin-wave theory of Ref. 31 is an approximation of the ground state of the Heisenberg model.⁴³

C. Band structure

The band structures of the AFM solutions are given in Fig. 6. The results show a wide gap (~ 17 eV) for both materials; we also see a similar large gap for the FM solutions. The experimental (optical) gap for La_2CuO_4 is about 2.0 eV.⁴⁴ That the gap is much larger than the experimental gap has been found much more generally in the HFA; see Refs. 12–14 for examples, and Ref. 12 for discussion. The results suggest that the insulating character of both materials is not strongly correlated with their magnetic ordering, in agreement with experiment,⁴⁵ and in contradiction to a band-theory scheme proposed in Refs. 15 and 46. In the La_2NiO_4 AFM solution, the Γ point of the highest occupied band consists mainly of the Ni $3d_{x^2-y^2}$ and O(1) $2p_{x,y}$, and the Γ point of the lowest unoccupied band consists mainly of the O(1) $3s$ and O(2) $3s$, plus a bit of Ni $4s$ and O(2) $3p_z$. In the La_2CuO_4 AFM solution, the Γ point of the highest occupied band consists mainly of the Cu $3d_{x^2-y^2}$ and O(1) $2p_{x,y}$, and the Γ point of the lowest unoccupied band consists mainly of the O(1) $3s$ and O(2) $3s$, plus a bit of Cu $4s$. For

both materials, the Γ point is the minimum in the lowest unoccupied band but not the maximum in the highest occupied band, showing an indirect band gap. The width of the highest occupied band is about 1.6 eV for La_2NiO_4 and 0.6 eV for La_2CuO_4 . The projected densities of occupied states (not shown) have many features in common with those previously reported HF results for other Mott insulators.^{12–14} Two of these features are that it is mainly anion p states that exist near the Fermi energy, and that the bulk of the magnetic ion e_g states is lower in energy than the t_{2g} states. These results are presently under analysis, and will be discussed further in a future publication.

III. SUMMARY AND DISCUSSION

We have calculated the electronic structure of La_2NiO_4 and La_2CuO_4 using the crystal HF approach. The major emphasis has been on ground-state properties, although some discussion of band structure has been given. The results provide supplementary information to that obtained from crystal LSDA and embedded-cluster calculations in interpreting the experimental data. For both materials, our crystal HF results correctly predict an AFM insulating ground state. The calculated Heisenberg exchange parameter J is about a factor of 3 too small compared with experiments. This is consistent with the interpretation of Martin and Illas,⁷ and Towler *et al.*¹²

that the HFA overestimates the on-site Coulomb interaction. The spin form factor $f(\vec{k})$ basically agrees with earlier cluster calculations. However, there is an appreciable discrepancy between the two theoretical calculations in the cuprate case, which we believe is due to the larger covalence in the cuprate. We found rough overall agreement with experiment for the shape of $f(\vec{k})$ vs $|\vec{k}|$ for a poor sample of the cuprate, and excellent agreement for the absolute intensity of the one Bragg reflection measured on a good cuprate sample. However in the case of La_2NiO_4 the shape of the form factors in both the crystal and cluster calculations disagree seriously with experiment. The fact that we found the nickelate to be (appreciably) less covalent than the cuprate deepens the puzzling nature of this disagreement with the nickelate together with agreement for the cuprate. For a further check, we also calculated the form factor for KNiF_3 , and found excellent agreement with experimental absolute intensities. These results should create strong motivation for performing more experiments on a stoichiometric sample of the nickelate; it is also important to measure the absolute Bragg intensities at more than one Bragg peak for a stoichiometric sample of La_2CuO_4 for a more stringent test of our theory.

We conclude with a discussion of the procedure used to calculate the spin density. We used our earlier result calculated within the single-band Hubbard model as a guide. That is, following that result, we took the spin density to be that in the HFA reduced by the ratio $\langle s_z \rangle_{\text{Heis}}/s$, the reduction from 1 being due to the quantum spin fluctuations in the Heisenberg AFM ground state. In fact, we have shown⁴⁷ that this procedure is not exact for a model more general than the single-band Hubbard model. Thus we need to understand, e.g., why our present and previous⁵ results are in excellent agreement with experiment for a number of cases using the HFA. Such studies are in progress. In any case, we want to emphasize that the QSF's (which give large effects) cannot be ignored, as they were in Ref. 10, where a large moment reduction was attributed entirely to covalence. We note also that, in Ref. 7, a large QSF correction was made, showing the confusion on this issue in the literature. The single-band Hubbard model result [Eq. (3)] is a good starting point for clarification, and the generalization is clearly important.

ACKNOWLEDGMENTS

We thank K. Kubo, D. J. Buttrey, and J. M. Honig for valuable discussions.

APPENDIX: ON THE DETERMINATION OF THE HEISENBERG J FROM ELECTRONIC STRUCTURE CALCULATIONS

In this appendix, we discuss the theoretical justification behind the commonly used mapping scheme mentioned in Sec. II A in estimating the Heisenberg exchange parameter J from *ab initio* electronic calculations. We assume that the problems under consideration have their low-lying states governed by a Heisenberg Hamiltonian. Of course, if a problem is simple enough, one can calculate J exactly (using standard quantum-chemistry techniques such as configuration interaction). For example, if one were actually dealing with two magnetic electrons, with a limited number of non-

magnetic electrons, one could in practice calculate the energies of the true lowest-energy eigenstates, singlet and triplet. Equating their energy difference to the difference in eigenvalues of the Heisenberg Hamiltonian, would then yield J . This approach has been used.^{48–50,8–10}

However, for more complicated systems, we are forced to make approximations. The mapping scheme to estimate J in Sec. II A has been used for years, in both HF and density-functional calculations. We have shown⁴⁷ that for some special cases, e.g., a single-band Hubbard model, J_{HF} defined by Eq. (2) equals J to the leading order in perturbation with small hopping; however, this does not hold in general (although one may obtain a contrary impression from some papers¹⁰). Still J_{HF} serves as a reasonable and well-defined estimation of J .

We now discuss the determination of J within density-functional theory approaches, which invoke the following procedure.^{21,51,52} One obtains a symmetry-broken (SB) solution for the Kohn-Sham determinant D_{KS} for the ‘‘antiferromagnetic’’ state and a triplet state (for simplicity, we discuss the case of one magnetic electron per magnetic site in a two-magnetic-site cluster). The triplet energy minus the SB AFM state energy is equated to the triplet energy minus the (average) energy of the SB spin state $\alpha(1)\beta(2)$ for the Heisenberg model, thereby obtaining a number for J .⁵³ Although making the correspondence ‘‘SB electronic state \leftrightarrow SB spin state’’ sounds reasonable, one must realize that *there is not a unique SB spin state, even in this simplest of cases*. The following spin state is SB for all values of $\mu \neq 0$ or ∞ :

$$\Omega_\mu = \frac{1}{\sqrt{2(1+\mu^2)}} \{ \alpha(1)\beta(2) - \beta(1)\alpha(2) + \mu[\alpha(1)\beta(2) + \beta(1)\alpha(2)] \}. \quad (\text{A1})$$

The expectation value of the Heisenberg energy is

$$J \langle \vec{S}_1 \cdot \vec{S}_2 \rangle = -\frac{J}{4} \frac{3-\mu^2}{1+\mu^2}. \quad (\text{A2})$$

If one used the *exact* density functional (DF), then the energies of the exact lowest triplet and singlet states would be obtained. The difference in these energies would be equated to the corresponding difference in Eq. (A2) with $\mu = 0$ and ∞ , and this would give the exact J . However, given an approximate DF, as in almost all applications, one is faced with the problem of what value of μ to use in Eq. (A2) for the SB AFM state. Many people^{21,51,52} take $\mu = 1$ without giving a reason. But there is a potential inconsistency in doing so: as one's approximate DF grows closer to the exact DF, continued use of $\mu = 1$ may lead to serious errors. Thus the appropriate value of μ to use is unknown.

A possible way out of this dilemma is as follows. From Eq. (A2) one obtains

$$\mu = \left(\frac{\langle \vec{S}^2 \rangle}{(2 - \langle \vec{S}^2 \rangle)} \right)^{1/2}, \quad (\text{A3})$$

where $\vec{S} = \vec{S}_1 + \vec{S}_2$. One could demand that $\langle \vec{S}^2 \rangle$ be equal to the expectation value of the square of the total electronic

spin in D_{KS} , thus determining μ via Eq. (A3). One should remember that there is no guarantee that D_{KS} is an eigenfunction of \vec{S}^2 or that the average value $\langle \vec{S}^2 \rangle$ in D_{KS} is correct, even for the exact D_{KS} , presenting a possible inconsistency in this approach. Also, how to generalize this mapping idea for determining the SB AFM spin state to more than two sites (two electrons) is not obvious, and remains to be investigated.

Interestingly, this idea raises a question about the standard mapping used for the HFA, where μ is taken to be 1 for the AFM spin state. For this two-site, two-electron, example, one can show easily that $\langle \vec{S}^2 \rangle_{D_{HF}} = 1 - \delta^2$, where D_{HF} is the HF determinant of the AFM state and δ is the overlap integral between the two localized orbitals. Since δ is usually quite small (<0.1), it is seen that this probably would make little difference.

- ¹W. E. Pickett, Rev. Mod. Phys. **61**, 433 (1989).
- ²G. Y. Guo and W. M. Temmerman, J. Phys. C **21**, L803 (1988).
- ³A. Svane, Phys. Rev. Lett. **68**, 1900 (1992).
- ⁴P. Wei and Z. Q. Qi, Phys. Rev. B **49**, 12159 (1994).
- ⁵T. A. Kaplan, H. Chang, S. D. Mahanti, and J. F. Harrison, in *Electronic Properties of Solids Using Cluster Methods*, edited by T. A. Kaplan and S. D. Mahanti (Plenum, New York, 1995), p. 73.
- ⁶T. P. Das, in *Electronic Properties of Solids Using Cluster Methods* (Ref. 5), p. 1.
- ⁷R. L. Martin and F. Illas, Phys. Rev. Lett. **79**, 1539 (1997).
- ⁸F. Illas, I. de P. R. Moreira, C. de Graff, O. Castell, and J. Casanovas, Phys. Rev. B **56**, 5069 (1997).
- ⁹I. de P. R. Moreira and F. Illas, Phys. Rev. B **55**, 4129 (1997).
- ¹⁰J. Casanovas, J. Rubio, and F. Illas, Phys. Rev. B **53**, 945 (1996).
- ¹¹R. Dovesi, V. R. Saunders, C. Roetti, M. Causà, N. M. Harrison, R. Orlando, and E. Aprà, *CRYSTAL95 User's Manual* (University of Torino, Torino, 1996).
- ¹²M. D. Towler, N. L. Allan, N. M. Harrison, V. R. Saunders, W. C. Mackrodt, and E. Aprà, Phys. Rev. B **50**, 5041 (1994).
- ¹³J. M. Ricart, R. Dovesi, C. Roetti, and V. R. Saunders, Phys. Rev. B **52**, 2381 (1995).
- ¹⁴M. D. Towler, R. Dovesi, and V. R. Saunders, Phys. Rev. B **52**, 10 150 (1995).
- ¹⁵S. Massidda, M. Posternak, and A. Baldereschi, Phys. Rev. B **46**, 11 705 (1992).
- ¹⁶R. W. G. Wyckoff, *Crystal Structures*, 2nd ed. (Interscience, New York, 1963).
- ¹⁷The official web site of the CRYSTAL program is <http://www.dl.ac.uk/TCS/Software/CRYSTAL>, which contains a collection of basis sets for various atoms suitable for crystal calculations.
- ¹⁸P. J. Hay and W. R. Wadt, J. Chem. Phys. **82**, 270 (1985).
- ¹⁹N. W. Winter and R. M. Pitzer, J. Chem. Phys. **89**, 446 (1998).
- ²⁰P. W. Anderson, in *Solid State Physics*, edited by F. Seitz and D. Turnbull (Academic, New York, 1963), Vol. 14, p. 99. The mapping scheme is mentioned on p. 166. Note also Anderson's discussion of Kondo's work on this subject, on the same page.
- ²¹L. Noodleman, J. Chem. Phys. **74**, 5737 (1981).
- ²²S. Chakravaty, in *High-Temperature Superconductivity*, edited by K. S. Bedell, D. Coffey, D. E. Meltzer, D. Pines, and J. R. Schrieffer (Addison-Wesley, New York, 1990).
- ²³G. Aeppli and D. J. Buttrey, Phys. Rev. Lett. **61**, 203 (1988).
- ²⁴S. Itoh, K. Yamada, M. Arai, Y. Endoh, Y. Hidaka, and S. Hosoya, J. Phys. Soc. Jpn. **63**, 4542 (1994).
- ²⁵G. Aeppli, S. M. Hayden, H. A. Mook, Z. Fisk, S-W. Cheong, D. Rytz, J. P. Remeika, G. P. Espinosa, and A. S. Cooper, Phys. Rev. Lett. **62**, 2052 (1989).
- ²⁶P. E. Sulewski, P. A. Fleury, K. B. Lyons, S-W. Cheong, and Z. Fisk, Phys. Rev. B **41**, 225 (1990).
- ²⁷The parameters in the effective one-band Hubbard models for La_2CuO_4 and La_2NiO_4 are similar [A. K. McMahan (private communication)].
- ²⁸X.-L. Wang, C. Stassis, D. C. Johnston, T. C. Leung, J. Ye, B. N. Harmon, G. H. Lander, A. J. Schultz, C.-K. Loong, J. M. Honig, Phys. Rev. B **45**, 5645 (1992).
- ²⁹S. Shamoto, M. Sato, J. M. Tranquada, B. J. Sternlieb, and G. Shirane, Phys. Rev. B **48**, 13 817 (1993).
- ³⁰M. T. Hutchings and H. J. Guggenheim, J. Phys. C **3**, 1303 (1970).
- ³¹P. W. Anderson, Phys. Rev. **86**, 694 (1952). For more recent calculations supporting Anderson's original results, see J. D. Deger and A. P. Young, Phys. Rev. B **37**, 5978 (1988); M. Gross, E. Sanchez-Velasco, and E. Siggia, *ibid.* **39**, 2484 (1989); G. Castilla and S. Chakravarty, Bull. Am. Phys. Soc. **37**, 447 (1992).
- ³²A form factor measurement was made on $\text{La}_2\text{NiO}_{4.125}$ by J. M. Tranquada, J. E. Lorenzo, D. J. Buttrey, and V. Sachan, Phys. Rev. B **52**, 3581 (1995). The result showed a similar flatness at small k , being somewhat smaller than the stoichiometric case. This is large doping; the spin ordering is radically changed.
- ³³In the face of this major overall disagreement, we investigated an exotic ground state based on mixing of the high- and low-spin states on the Ni^{+2} , that could occur if the tetragonal structure caused a sufficiently large splitting between the two e_g states [Kaplan *et al.*, in *Electronic Properties of Solids Using Cluster Methods* (Ref. 5)]. Unfortunately, the state obtained did not correct the form factor at the important, small- k , Bragg peaks [T. A. Kaplan and S. D. Mahanti (unpublished)]; this was actually consistent with the small- e_g splitting found theoretically [A. K. McMahan (private communication)].
- ³⁴T. Freltoft, G. Shirane, S. Mitsuda, J. P. Remeika, and A. S. Cooper, Phys. Rev. B **37**, 137 (1988).
- ³⁵T. A. Kaplan and S. D. Mahanti, J. Appl. Phys. **69**, 5382 (1991).
- ³⁶K. Yamada, E. Kudo, Y. Endoh, Y. Hidaka, M. Oda, M. Suzuki, and T. Murakami, Solid State Commun. **64**, 753 (1987).
- ³⁷The arguments of Ref. 35 and in *Electronic Properties of Solids Using Cluster Methods* (Ref. 5) are empirical. A plausible rationale for the conclusion is the following. If there is an oxygen deficiency, there should be some Cu^{+1} , which simply dilutes the localized Heisenberg spins with nonmagnetic sites, leading to a reduction in the AFM moment and T_N . On the other hand, excess oxygen goes in interstitial positions located within the La_2O_2 bilayers as in the nickelate [D. E. Rice and D. J. Buttrey, J. Solid State Chem. **105**, 197 (1993)]; rather than causing Cu^{+3} , it causes O^{-1} in the CuO_2 planes, as is known for

- YBa₂Cu₃O_{6+δ}. But such an ion between two Cu⁺² causes a ferromagnetic interaction [T. A. Kaplan, Nucl. Phys. B (Proc. Suppl.) **5A**, 151 (1988); A. Aharony, R. J. Birgeneau, A. Coniglio, M. A. Kastner, and H. E. Stanley, Phys. Rev. Lett. **60**, 1330 (1988)], so this tends again to make the AFM moment and T_N decrease on adding oxygen to the stoichiometric material.
- ³⁸B. Keimer, A. Aharony, A. Auerbach, B. J. Birgeneau, A. Casanholo, Y. Endoh, R. W. Erwin, M. A. Kastner, and G. Shirane, Phys. Rev. B **45**, 7430 (1992).
- ³⁹In *Electronic Properties of Solids Using Cluster Methods* (Ref. 5), the spin reduction for La₂CuO₄ is larger than this 15.8%. We believe the main source of the difference lies in the different definitions used.
- ⁴⁰J. Hubbard and W. Marshall, Proc. Phys. Soc. London **86**, 561 (1965).
- ⁴¹This is qualitatively consistent with parameters in the multiband models as calculated by A. K. McMahan using constrained local density calculations. He finds [see *Electronic Properties of Solids Using Cluster Methods* (Ref. 5), p. 157] that the charge-transfer energy ϵ_{pd} is appreciably larger in the nickelate than the cuprate, while the hopping parameter t_{pd} is very similar in the two cases (private communication).
- ⁴²Some of the present authors had accepted this: T. A. Kaplan, S. D. Mahanti, and H. Chang, Phys. Rev. B **45**, 2565 (1992).
- ⁴³Comparison with experiment of the “magnetic moment” m calculated in the HFA for MnO and NiO was made in the course of calculations similar to ours, by M. D. Towler *et al.* (Ref. 12). We point out that their discrepancies ($m_{\text{theor}} > m_{\text{expt}}$) would be reduced if the quantum spin fluctuations were taken into account (as they should be, in principle, according to our argument above). Also, replacing their use of the Mulliken spin population by the Hubbard-Marshall (HM) extrapolation (Ref. 40) would go in the direction of decreasing the theoretical moment. That the HM theory is more appropriate for comparison with neutron diffraction results was discussed by S. D. Mahanti, T. A. Kaplan, H. Chang, and J. F. Harrison, J. Appl. Phys. **73**, 6105 (1993). The best procedure for comparing theory and experiment is to consider the measured quantities and the intensities of the Bragg peaks (as we have done above) directly, avoiding perhaps controversial questions of how to define the antiferromagnetic moment.
- ⁴⁴S. L. Cooper, G. A. Thomas, A. J. Millis, P. E. Sulewski, J. Orenstein, D. H. Rapkine, S-W. Cheong, and P. L. Trevor, Phys. Rev. B **42**, 10 785 (1990).
- ⁴⁵D. Adler, in *Solid State Physics*, edited by F. Seitz, D. Turnbull, and E. Ehrenreich (Academic, New York, 1968), p. 1.
- ⁴⁶J. C. Slater, Phys. Rev. **82**, 538 (1951).
- ⁴⁷T. A. Kaplan, S. D. Mahanti, Y.-S. Su, and J. F. Harrison (unpublished).
- ⁴⁸J. Hubbard, D. E. Rimmer, and F. R. A. Hopgood, Proc. Phys. Soc. London **88**, 13 (1966).
- ⁴⁹D. E. Rimmer, J. Phys. C **2**, 329 (1969).
- ⁵⁰A. B. van Oosten, R. Broer, and W. C. Nieuwpoort, Chem. Phys. Lett. **257**, 207 (1996).
- ⁵¹F. Illas and R. L. Martin, J. Chem. Phys. **108**, 2519 (1998).
- ⁵²R. Caballol, O. Castell, F. Illas, I. de P. R. Moreira, and J. P. Malrieu, J. Phys. Chem. **101**, 7860 (1997).
- ⁵³In an earlier work, Heisenberg exchange constants (J) are also obtained by making a correspondence between Kohn-Sham determinants and product spin states [T. Oguchi, K. Terakura, and A. R. Williams, Phys. Rev. B **28**, 6443 (1983)], with no mention of symmetry breaking.